Traceable Calibration of Power Quality Standards

Speaker: Waldemar G. Kürten Ihlenfeld
Authors: Waldemar G. Kürten Ihlenfeld[1] and Ricardo Iuzzolino[2]
[1)] Physikalisch-Technische Bundesanstalt,
Bundesallee 100, D-38116 Braunschweig,
Germany
Tel.: +49 531 592 2374, Fax: +49 531 592 2305
email: guilherme.ihlenfeld.@ptb.de
[2)] Instituto Nacional de Tecnologia Industrial
Av. General Paz 5445 Casilla de Correo 157
B1650WAB San Martin, Buenos Aires, Argentina
email: ricardo.iuzzolino@inti.gov.ar

Abstract

The demand of electric energy is soaring worldwide and this tendency will persist in the future. The deregulation of electricity markets has urgently been asking for enhanced traceability of calibrations in the field of electric power and energy. The industry heeding to these claims placed modern electrical power standards into the market, which are able to synthesize complex alternating signals (ac) and power quality parameters in compliance with IEC power quality standards. These devices pose stringent calibration demands. In order to attend these needs, much effort at the National Metrology Institute of Germany (Physikalisch-Technische Bundesanstalt – PTB) has been devoted to the development of novel and more accurate measurement methods of electric power and energy, and ultimately of power quality parameters, especially of highly distorted waveforms.

Evidences suggest that, at the PTB, ac power in the range of power frequencies can nowadays be determined with measurement uncertainties typically around few μW/VA using elaborated digital sampling techniques [1,2]. A thorough derivation of measurement uncertainties of the spectral lines of a discrete Fourier Transform forms the basis for inferring the measurement uncertainty of harmonics determined from digital sampling.

The PTB primary power standard used to do the most accurate measurements in laboratory has been enhanced in order to guarantee traceability of ac power to the SI (Système International d'unités) in the range of frequencies from direct current (dc) to around 5 kHz. Therefore, power standards for power quality parameters (like harmonics, flicker, fluctuating harmonics, and inter-harmonics) can be calibrated with measurement uncertainties as low as some tens of parts in one million.

1. Introduction

The PTB sampling system [2,3] for calibrating power quality standards is depicted in figure 1. The device under test (DUT – e.g., a Fluke 6100A standard) can be programmed to synthesize signals with different harmonic content, flicker, modulating harmonics and interharmonics. Its output voltage is connected to either a resistive divider or a voltage transformer (with a nominal ratio $\underline{K}_v$) to reduce it to measurable levels (lower than 7 V effective.) The output voltage of the transformer $\underline{U}_1$ is connected to the first channel of the signal switch (CH1). The output current of the source is connected to the primary of a current transformer (with nominal ratio $\underline{K}_i$) with its secondary connected to an ac shunt ($\underline{Z}$) resulting in an output

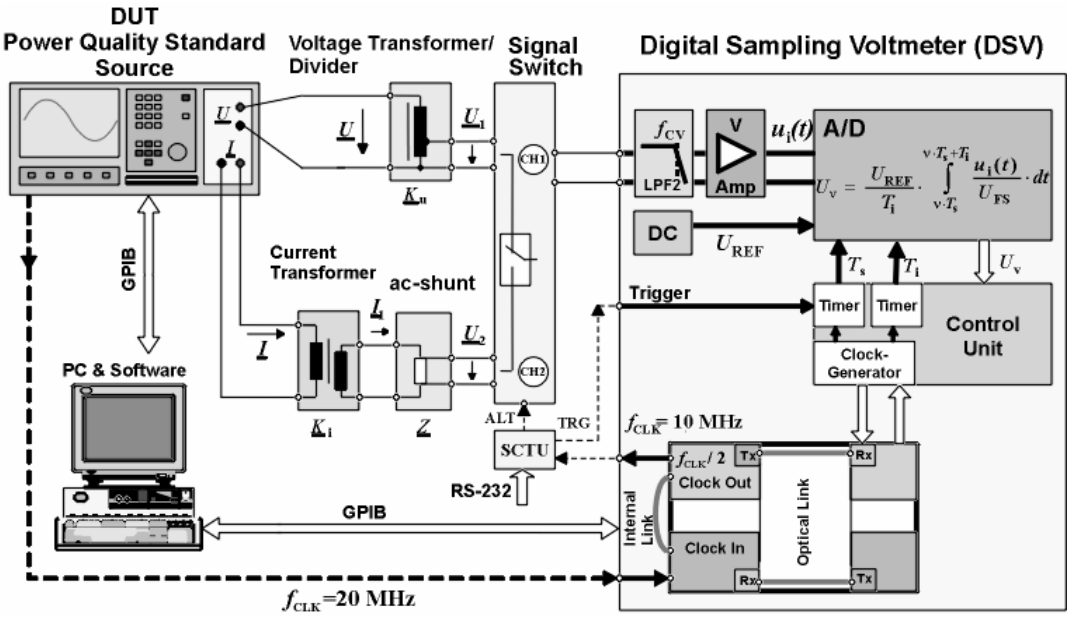

Figure 1. PTB Measuring system setup for power quality calibrations.

voltage $\underline{U}_2$ across its terminals (CH2). A duplex (two-way) optical link using high-speed optical transmitters and receivers was built inside the DSV (at the right in figure 1) to provide a clock reference to its internal 28-bit integrating analog-to-digital converter (ADC). The kernel of the system is the DSV with its internal reference U_{REF} and of full-scale U_{FS} operating in the dc sampling mode with T_s standing for the sampling time and T_i for the aperture time. Its input stage is represented by an analog filter with cutoff frequency f_{cv} and an amplifier with gain V nearly equal to one. The high magnitude signals $\underline{U}$ and $\underline{I}$ are conditioned by a voltage- and current transformer with a shunt $\underline{Z}$ of known frequency response.

In the optical path, the clock signal f_{CLK} (20 MHz) of the source is divided by two resulting in a 50% duty-cycle 10 MHz clock reference, which is fed to a synchronous counter and trigger unit (SCTU) for controlling the signal switch and triggering of the DSV. The SCTU counts the number of periods of the synthesized waveforms (coherent to f_{CLK}) of the source enabling the switch to alternately select the signals (via ALT pulses) at its channel-inputs (CH1 and CH2) to be sampled by the DSV. In addition, the SCTU provides trigger pulses (TRG) at a rate T_s (sampling interval) to the DSV that samples the signals synchronously with the reference clock of the source. This is of utmost importance in order to reach higher accuracy levels during the ac sampling process and to prevent DFT leakage and to sensibly reduce timing jitter effects [4].

In the absence of an external synchronizing clock frequency from the DUT, the optical link automatically selects the internal time-base of the DSV as the reference clock for the measurement system. The PC compatible computer controls the DUT, gathers the DSV data, process the discrete Fourier transform (DFT) on samples and computes the power quality parameters.

2. Model of the Sampler

The sampled voltage $U_v = U(t) = U(v \cdot T_s)$ (i.e., at a time $t = v \cdot T_s$) of an integrating ADC internal to the DSV is the mean value of the signal over a time span T_i and may be stated as

$$U(\nu \cdot T_s) = \frac{1}{T_i + \varepsilon_{JTi}} \left(1 + \varepsilon_{REF} + \varepsilon_G + \frac{\varepsilon_{LIN} + \varepsilon_{RES}}{Abs[U_v]} U_{FS} \right) \int_{\nu \cdot T_s + \varepsilon_{JTs}}^{\nu \cdot T_s + \varepsilon_{JTs} + T_i + \varepsilon_{JTi}} [u(t) + u_S(t)] dt + u_{sn}(\nu \cdot T_s) \quad (1)$$

where

$$Abs[U_v] = |U(v \cdot T_s)|_{\varepsilon_G = \varepsilon_{REF} = \varepsilon_{LIN} = \varepsilon_{RES} = \varepsilon_{JTi} = \varepsilon_{JTs} = 0} \quad (2).$$

The variables ε_{REF}, ε_G, ε_{LIN}, ε_{RES} represent deviations in respect to the internal dc reference, deviation of gain, linearity and deviation due to the finite resolution of the DSV (normalized to the full scale U_{FS}). The variables ε_{JTs} and ε_{JTi} stand for time-jitter effects of the sampling time T_s and aperture time (or integration time) T_i. Inside the integral representing the high-resolution ADC the quantity $u_S(t)$ represent noise components produced in the source and $u_{sn}(t)$ stands for sampling noise produced by the sampling voltmeter. Table 1 summarizes the random variables of eq. (1).

Table 1

VARIABLES	DESCRIPTION	PROBABILITY DENSITY FUNCTION	LIMITS OF THE DISTRIBUTION/OR VARIANCE	CORRELATION AMONG SAMPLES
ε_{REF}	deviation due to calibration uncertainty of the internal DC reference voltage of the sampling voltmenter	rectangular	0.5 μV/V	Yes, because it remains constant when taking all samples (see ref. 2)
ε_G	deviation due to gain errors of the internal ADC of the sampling voltmeter	Gaussian	INT(0.002/T_i[s]) and clamped at max 30 μV/V	Yes (see ref. 2)
ε_{RES}	random variable representing loss of resolution due to quantization. It is dependent on T_i and related to the full scale value U_{FS}.	rectangular	ex.: at Ti = 975 μs its value is 0.15 μV/V	No, because it may change from sample to sample. (see ref. 2)
ε_{LIN}	random variable representing deviations due to linearity (mainly integral) related to the full scale value	rectangular	0.1 μV/V	No. Experiments show it is also variable (see ref. 2)
ε_{JTs}	random variable representing jitter of the sampling time	rectangular	5 ns (was overestimated because of additional circuitry, normally around 100 ps)	No (see ref. 2)
ε_{JTi}	random variable representing jitter of the aperture (or integration) time	rectangular	5 ns	No (see ref. 2)
$u_s(t)$	Noise component of the source	Gaussian	expressed by its noise power density spectrum	No (see ref. 2)
$u_{sn}(t)$	Sampling noise of the sampling voltmeter	Gaussian	$0.81 \cdot \left(\frac{0.001}{T_i[s]} \right) \cdot U_{FS}^2$ $(\mu V)^2$	No (see ref. 2)

The sampling process of $u(t)$ is accomplished under the following constraints:

1. The condition for the sampling time $T_s = 1/(N f_o)$ must hold at all times for N an integer. This is the condition for synchronous sampling of a signal with the fundamental frequency f_o derived from a common clock-reference.
2. The number of sampled periods M must be an integer multiple of power-line cycles in order to reduce power-line interferences. Conditions 1 and 2 prevent artificial spectral components (leakage) from appearing on a DFT on sampled data.

The suppression of harmonics of the power-line frequency occurs when $1/(T_i f_o) >> 1$ and integer. On the set of $L = M \cdot N$ samples $U(\nu \cdot T_a)$ a DFT can be expressed by the function $DFT(\mathrm{j}\omega_k)$ as

$$DFT(\mathrm{j}\omega_k) = \frac{2}{L} \cdot \sum_{\nu=0}^{L-1} \frac{U(\nu \cdot T_s)}{\sin\left(\frac{\pi T_i \cdot k}{N \cdot T_s}\right) / \left(\frac{\pi T_i \cdot k}{N \cdot T_s}\right)} \cdot e^{-\mathrm{j}\omega_k \nu \cdot T_s} \cdot e^{-\mathrm{j}\left(\frac{\pi T_i \cdot k}{n \cdot T_s}\right)} \quad (3),$$

where

$$\omega_k = \frac{2\pi}{L \cdot T_s} \cdot k \qquad \text{for} \qquad k = 0, 1, ..., L\text{-}1 \quad (4).$$

Equation (3) accounts for phase and amplitude correction of each spectral line at ω_k due to a finite aperture time T_i, as expressed by the $\sin(x)/x$ function in its denominator and the last exponential at the right.

3. Noise Issues

In order to access measurement uncertainties of ac quantities inferred from digitally sampled data and Fourier transform it is of fundamental importance to understand interfering effects on signal generation as well as on digital acquisition by sampling. These disturbing effects may be classified as 'noise' imposing ultimate limits on measurement uncertainties. Noise may be classified, for our purpose, into two categories: (a) noise contributions correlated with the sampling process or of 'clock-coherent' nature and ultimately with the sampling frequency f_s (called 'spurious'), and (b) noise components uncorrelated with the signal.

3.1. Correlated Noise

Frequency correlated noise sources generally produces systematic deviations on data obtained by digital sampling. Their effects are difficult to estimate, often demanding laborious mathematical modeling [3,5].

Synchronization between source and sampler as shown in figure 1 reduces time jitter effects but inevitably introduces synchronous aliasing components (spurious) that may produce systematic errors (or aliasing) when these components are located beyond the Nyquist frequency $1/(2\ T_s)$ of the sampler. These errors are caused by side-band harmonics, DAC quantization, glitches or spikes during DAC step transitions, clock-feedthrough, DAC's differential and integral nonlinearity, clock delay instabilities and clock jitter. These effects will be dealt with in more detail at the workshop.

Side-band harmonics are inherent to signal synthesis and are located at multiples of the clock or update rate frequency of the DAC i.e., at f_{clk}-f_o, f_{clk}+f_o, 2 f_{clk}-f_o, 2 f_{clk}+f_o and so forth, always separated by $\pm f_o$. The higher the number of steps when synthesizing the signal, the higher

must be f_{clk}. These harmonics can be partially removed by a low-pass (LP) antialiasing filter, which helps attenuating DAC quantization noise too.

Quantization produces higher order odd harmonics and cause biasing (systematic deviations) on a DFT applied on samples [7]. The problem of quantization noise is object of extensive analysis [7-8].

Spikes or glitches are mainly produced by charge injection and time delays in analog switches internally in a DAC. Time-delayed sample and hold amplifiers may further alleviate this problem.

Clock-feedthrough makes itself perceptible by the presence of exponentially decaying (generally resembling a sinusoidal pattern of very high frequency) whose repetition-rate is coherent to the main clock. A LP-filter is used to mitigate its effects.

Differential and integral nonlinearities of the DAC present a wide spectrum of odd harmonics very similar to that from quantization. Evaluation of their effects seems to be possible by a statistical treatment assuming a constant power density spectrum homogeneously distributed over the entire Nyquist bandwidth of the DAC (from dc to $f_{clk}/2$).

Generally clock delay, as long as it remains stationary, does not impair measurements by digital sampling. Clock jitter of the order of nanoseconds though, increases signal-to-noise ratio (SNR), which becomes pronounced (i.e., < 120 dB) at fundamental frequencies f_o greater than around 500 Hz. A detailed treatment of such noise sources is outside the scope of this article. The reader should refer to [3] for further details on estimating systematic deviations produced by signal synthesis correlated noise.

3.2. Uncorrelated Noise

Uncorrelated noise components are those contributions of random nature arising from thermal and flicker noise, i.e., intrinsic noise of electronic components in the measuring circuitry. These noise contributions are present in the ac voltage source and in the DSV circuitry as well. Since the digital sampling spans over a large number of samples (or single random variables), according to the central limit theorem, the resulting random variable given by the sum of random variables with a finite auto-correlation function is also a random variable with an asymptotic Gaussian distribution [5,6].

Noise is band-limited by the low-pass (LP) filter at the output of the source and by filters inside the DSV. The DSV filters the input signal noise with an internal analog LP filter with cutoff frequency f_{CV} and further attenuates it due to its integrating characteristics (digital filtering). In this case the white noise bandwidth BW_n depends only on the aperture time and it establishes the theoretical resolution limit of the ADC as

$$BW_n = \frac{1}{2T_i} \tag{6}.$$

Additional noise arises from internal switching mechanisms inside the DSV totalized as sampling noise, whose rms contribution is estimated according to the equation of the last line inn the 4th row of table 1.

Noise contributions from the source are normally expressed by a noise power spectral density $S(f)$ (in nV/√Hz) as

$$S(f) = \frac{K_f}{\sqrt{f}} + S_n \tag{7},$$

where K_f stands for a colored or flicker noise coefficient (usually expressed in nV) and S_n for the ground white-noise spectral density. $S(f)$ can easily be estimated [9] by sampling a noise signal $n(t)$ during an observation window of length $L = MN$ samples obtained at a rate T_s according to

$$S^2(f_k) \approx \frac{|F(j\omega_k)|^2 T_s}{L} \tag{8},$$

where $F(j\omega)$ is the discrete Fourier transform redefined here as

$$F(j\omega_k) = \sum_{v=0}^{L-1} n(vT_s) e^{-j\omega_k v T_s} \tag{9}.$$

The rms-noise voltage U_n may thus be expressed as

$$U_n = \sqrt{\int_{-\infty}^{+\infty} S^2(f) df} \approx \sqrt{\sum_{k=0}^{L-1} \frac{|F(j\omega_k)|^2 T_s}{L} \cdot \left(\frac{1}{LT_s}\right)} = \sqrt{\sum_{k=0}^{L-1} \left|\frac{F(j\omega_k)}{L}\right|^2} \tag{10}$$

This means that white noise with a total variance U^2_n measured over a certain bandwidth would contribute to the variance $s^2_{DFT}(\omega_k)$ of the DFT as defined in (3) either for the real or imaginary parts as

$$\left\{ \begin{array}{l} s^2_{DFT}(\omega_k) = \frac{2}{L} U_n^2 \quad for \quad k \neq 0; \\ s^2_{DFT}(0) = \frac{1}{L} U_n^2 \quad for \quad k = 0 \ or \ DC; \end{array} \right\} \tag{11}$$

Conversely, the determination of the effect of noise on the spectral components of a DFT demands knowledge of the noise auto-correlation function. White noise does not produce covariances between pairs of DFT spectral components at frequencies f_i and f_j (for $f_k = k/(LT_s)$ and $i \neq j$) and no correlation between any DFT real and imaginary parts. Colored noise, however, do produce correlation [5] between the spectral components i and j. The covariances among spectral lines can in most practical cases be neglected without any loss of accuracy because their magnitude are, often by many orders of magnitude smaller than the variances of each spectral line. This procedure substantially simplifies the analysis of noise contributions and will be adopted here.

Assuming noise information as in eq. (7) is valid for positive frequencies (one-sided noise power density) the summation in eq. (10) is done for $k = \{0,\ldots,L/2 - 1\}$. The corresponding noise contributions to the DFT spectral lines (as defined by eq. (3)) for the real $s^2_{DFTRe}[k]$ or imaginary parts $s^2_{DFTIm}[k]$ may thus be estimated from

$$s^2_{DFT\,Re}[k] = s^2_{DFT\,Im}[k] = \frac{S^2\left(\frac{k}{LT_s}\right)}{LT_s} \tag{12}$$

In case K_f is specified as usual in nV and S_n in nV/√Hz, the noise contributions in $(\mu V)^2$ are

$$s^2_{DFT\,Re}[k] = s^2_{DFT\,Im}[k] = \frac{S_n^2}{10^6} \cdot \frac{1}{LT_s} + \frac{K_f^2}{10^6} \cdot \frac{1}{k} \tag{13},$$

for $k \neq 0$;

4. Evaluating Uncertainty of DFT Spectral Components

Evaluations of measurement uncertainties of sampling systems remain valid if and only if frequency components at and above half the sampling frequency are attenuated to a level below the dynamic range of the sampler in order to avoid systematic deviations produced by aliasing. This relies on the "correct use" of sampling techniques, otherwise no uncertainties could be predicted. In this case, the most important parameters to consider are ε_{REF} and ε_G of the sampler since correlation among each sampled value annihilates any reduction of uncertainties from averaging many estimations of U_{eff}.

Uncertainty evaluations are firstly done by assuming sinusoidal signal components with a peak value U_m and period T_o at the input of the DSV (although $u(t)$ may be of any waveform):

$$u(t) = U_m \sin(\frac{2\pi}{T_o} t) \tag{14}.$$

In order to further simplify variable indexing, the variables of Table 1 are renamed as:

$$\begin{Bmatrix} q_1 = \delta_{REF} \\ q_2 = \delta_G \\ q_3 = \delta_{RES} \\ q_4 = \delta_{LIN} \\ q_5 = \delta_{JTo} \\ q_6 = \delta_{JTs} \\ q_7 = \delta_{JTi} \end{Bmatrix} \tag{15}$$

The sensitivity coefficients of each sample U_v in respect to any q_m (for m = 1, … ,7 as above) are

$$c_{vm} = \frac{\partial U_v}{\partial q_m} \tag{16},$$

and the covariance $u(U_v, U_k)$ between the sampled value v and k is expressed as

$$u(U_v, U_k) = \sum_{m=P}^{Q} c_{vm} c_{km} u^2(q_m) \tag{17},$$

where P and Q are integers from 1 to 7 for indexing the q_m, which produce correlation. For example, if only q_1 and q_2 produce correlation among samples, $P = 1$ and $Q = 2$;

Splitting the DFT in its real and imaginary components $DFT\mathrm{Re}[k,v]$ and $DFT\mathrm{Im}[k,v]$ respectively, their sensitivity in respect to each sampled value U_v are:

$$c\,\mathrm{Re}[k,v] = \frac{\partial DFT\,\mathrm{Re}[k,v]}{\partial U_v} \tag{18}$$

$$c\,\mathrm{Im}[k,v] = \frac{\partial DFT\,\mathrm{Im}[k,v]}{\partial U_v} \tag{19}$$

The uncertainties for the real and imaginary parts of the DFT can thus be straightforwardly expressed as

$$u^2 DFT\,\mathrm{Re}[k] = \sum_{v=0}^{L-1} c\,\mathrm{Re}[k,v]^2 \sum_{m=1}^{7} c_{zm}^2 u^2(q_m) + 2\sum_{w=0}^{L-2}\sum_{p=w+1}^{L-1} c\,\mathrm{Re}[k,w]\cdot c\,\mathrm{Re}[k,p]\cdot u(U_w, U_p) + s^2_{DFT\,Re}[k] \tag{20}$$

$$u^2 DFT\,\mathrm{Im}[k] = \sum_{\nu=0}^{L-1} c\,\mathrm{Im}[k,\nu]^2 \sum_{m=1}^{7} c_{zm}^2 u^2(q_m) + 2\sum_{w=0}^{L-2}\sum_{p=w+1}^{L-1} c\,\mathrm{Im}[k,w]\cdot c\,\mathrm{Im}[k,p]\cdot u(U_w,U_p) + s_{DFT\,Im}^2[k] \tag{21}$$

Key values for calculating uncertainties are the $u^2(q_m)$ (variances or limits in the 4th column of table 1) and the sensitivity coefficients. Variance contributions due to sampling noise u^2_{sn} in $(\mu V)^2$ must be further included in eqs. (20) (21) (note that v runs from 1 to 7, i.e., from $q_1 = \varepsilon_{REF}$ to $q_7 = \varepsilon_{JTi}$). Its variance contribution due to sampling noise (assumed of white nature) is first multiplied by $2/L$ as in eq. (11):

$$u_{sn}^2 = \frac{2}{L}\cdot 0.81\cdot\left(\frac{0.001}{T_i[s]}\right)\cdot U_{FS}^2 \tag{22},$$

and summed to the right terms of eqs. (20) and (21). Once the uncertainties of the spectral lines are known, the uncertainty of the effective value, as defined in eq. (5), can be obtained with further application of the GUM (Guide to the Expression of Uncertainty in Measurements.)

The equations above were extended for the evaluation of uncertainties of distorted waveforms implemented in a program (written in Borland C++Builder) called SAM (acronym of SAMpled Data Uncertainty Evaluation Program). This program is used to evaluate type B uncertainties of the PTB primary sampling ac power standard. Included in the program is the calculation of uncertainties for the ratio of DFT spectral lines, an important quantity for determining besides ac power, impedances (resistance, capacitance, inductance, phase and time-constant of resistors and shunts) as well.

The uncertainty model for the sampler in the system of figure 1 was validated by replacing the digital source with a Josephson ac voltage synthesizer [10], which is able to synthesize low-noise ac signals with fundamental (quantum) accuracy. Experimental evidence corroborates the premises of the model established by the DSV.

Future investigations with quantum standards will allow the PTB to maintain the traceability and maintenance of ac quantities by digital sampling with uncertainties bearing the 1 μV/V from dc up to around 1 kHz.

5. Flicker Measurements

Calibration power calibrators in respect to flicker according to the IEC standards [11,12] demand the accurate determination of modulation factors. Modulation measurements described in this paper were done fundamentally in the frequency domain as described next. Short-term flicker severity P_{st} depends on the modulation factor and on the frequency of the modulating signal according to table 5 in section 5 in the IEC-61000-4-15 standard [11].

5.1 Sinusoidal Modulation

This is the straightforward case and the modulation factor can easily be obtained from the spectrum of the sampled signal as:

$$m = 2\frac{\left(A_{LSB} + A_{USB}\right)}{A_0} \tag{23},$$

where A_{LSB}, A_{USB} and A_0 are the root-mean-square (rms) values of the lower side-band, upper side-band and fundamental respectively, obtained from the DFT.

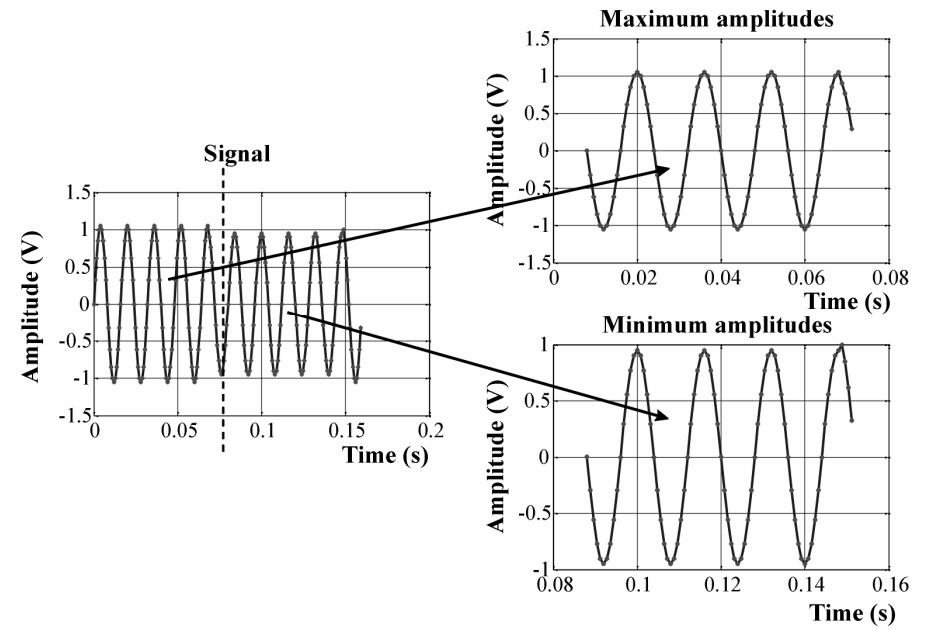

Figure 2. Square wave modulated signal. The frames are used separately to obtain the modulation factor after applying the DFT on each group of frame samples. Each frame has an integer number of periods of the signal.

5.2 Rectangular Modulation

The rectangular modulation introduces odd harmonics that demand higher sampling rates to prevent aliasing when determining the modulation factor from samples. Therefore, the modulation factor is best obtained from the spectrum (or DFT) using the time domain windowing technique over an observation window of M periods of the fundamental encompassing an integer number P of periods of the modulating frequency.

In this case, the modulation factor is computed as

$$m = 2\left(\frac{A_{\mathrm{MAX}} - A_{\mathrm{MIN}}}{A_{\mathrm{MAX}} + A_{\mathrm{MIN}}}\right) \qquad (24),$$

where A_{MAX} and A_{MIN} are the maximum and minimum peak values respectively.
In the case presented here, rms values were used instead of peak values. The signal is split in observation frames (windowing technique) containing samples related to the portion of the signal with constant amplitudes (A_{MAX} and A_{MIN}). This has been accomplished by using a program written in C++ to sort the data properly in order to prevent DFT leakage. Then the DFT is applied to the M-1 periods contained in each of these frames (M-1 and not M periods in order to firstly avoid discontinuities of the transition due to rise and fall times of the modulation and a fractional number of cycles). This procedure is illustrated in Fig. 2. The rms values of the fundamental frequency are obtained from the DFT, and m is calculated from (24).

Table 2 summarizes the calibration results using the method described in this section. Two different modulation factors of 10 % and 0.402 % with f_{m} = 6.25 Hz were used with the fundamental frequency at 62.5 Hz. The results show that the deviation from the nominal setting (10 % and 0.402 %) is smaller than 1 % (relative to m). The 3rd, 4th and 7th columns show evaluated type B uncertainties for a coverage factor k = 1.

Table 2
SQUARE-WAVE MODULATION RESULTS USING THE WINDOWING TECHNIQUE

m nom (%)	Calculated m	Unc. (10E-6)	Unc. relative (10E-6)	Deviation (%)	Ampl. of the fundamental A_0		Unc. (10E-6)
0.402	0.004022	8.9	2227.2	0.0002	5.00071	A	5.9
10	0.100006	8.9	89.1	0.0006	5.00065	A	5.9
0.402	0.0040167	1.7	434.2	-0.0003	100.00289	V	0.9
10	0.1000026	1.6	15.7	0.0003	100.00262	V	0.9
10	0.0999995	5.9	59.8	0.0000	109.9999	V	7.8

6. Fluctuating Harmonics

The phenomenon of fluctuating harmonics arises when one or more harmonic frequencies of the fundamental frequency fluctuate. In this case the short time Fourier transform (STFT) [13,14] may be applied on samples. For the synchronous system, the fluctuating harmonics can be analyzed in a similar way as flicker at either sinusoidal or rectangular modulation.

The modulation factor can be computed from the spectrum as follows,

$$m = \frac{A_{\mathrm{LSB}} + A_{\mathrm{USB}}}{A_{\mathrm{h}}} \qquad (25),$$

where A_{LSB}, A_{USB} and A_{h} are the rms values of the lower side-band, upper side-band and harmonic respectively.

The same methods apply for the rectangular modulation, which are valid for flicker to compute the modulation factor m.

7. Interharmonics

An interharmonic is a frequency component not an integer multiple of the fundamental frequency [15]. This phenomenon can be analyzed as a special case of harmonic component measurement (since the very same time-base clock locks source and sampler). Not all interharmonics can be calibrated with the synchronous sampling system. As in the case of flicker, the observation window must encompass both an integer numbers of periods of the fundamental and of the interharmonic.

Extensive numerical simulations corroborated by experimental evidence suggest that the synchronous sampling technique can successfully be used to calibrate the most demanding power quality sources (calibrators). The calibration done at the PTB demonstrates that measurement uncertainties are of some parts in 10^6.

References:

1. F. J. J. Clarke and J. R. Stockton, “Principles and Theory of Wattmeters Operating on the Basis of Regularly Spaced Sample Pairs,” *J. Phys. E*, vol. 15, pp. 645-652, 1982.

2. Ramm, G.; Moser H.; Braun, A., “A New Scheme for Generating and Measuring Active, Reactive and Apparent Power at Power Frequencies with Uncertainties of 2.5 10-6”, *IEEE Trans. on Instrum. Meas.*, vol. 48, pp. 422-426, No. 2, April 1999.

3. W. G. Kürten Ihlenfeld, “Maintenance and Traceability of AC Voltages by Synchronous Digital Synthesis and Sampling”, PTB-Report E-75, August 2001.

4. W. G. Kürten Ihlenfeld, E. Mohns, H. Bachmair, G. Ramm, and H. Moser, “Evaluation of the synchronous generation and sampling technique,” IEEE Trans. Instrum. Meas., vol. 52, no. 2, pp. 371-374, Apr. 2003.

5. J. Schoukens and J. Renneboog, ”Modeling the noise influence on the Fourier coefficients after a discrete Fourier transform,” *IEEE Trans. Instrum. Meas*., vol 35, No.3, pp 278-286, September 1986.

6. A. Papoulis, *Probability, Random Variables and Stochastic Processes,* McGraw-Hill, 1991.

7. M. F. Wagdy, “Effect of ADC quantization errors on some periodic signals measurements,” *IEEE Trans. Instum. Meas.,* vol. 36, No. 4, pp 983-989, December 1987.

8. R. M. Gray, “Quantization Noise Spectra“, *IEEE Trans. Inf. Theory,* vol. 36, No. 6, pp. 1220-1244, November 1990.

9. W. G. Kürten Ihlenfeld, “Tutorial on noise,” *Lecture of the III. Conference on Electrical Metrology, III Semetro*, Rio de Janeiro, Brazil, Spetember 1998.

10. W. G. Kürten Ihlenfeld et al., “Characterization of a high-resolution analog-to-digital converter with a Josephson ac voltage source,” *IEEE Trans. Instrum. Meas.*, vol. 54, No.2, pp 649-652, April 2005.

11. IEC-61000-4-15, Electromagnetic compatibility (EMC), Part 4: Testing and measurement techniques – Section 15: Flickermeter – Functional and design specifications.

12. IEC 868-0, Technical Report, Part 0: Evaluation of flicker severity.

13. Paul Wright, “Calibration of Power Frequency Harmonics Analysers as used in Conjunction with EN61000-3-2”, National Physical Laboratory, NPL, Queens Road, Teddington, UK.

14. IEC-61000-4-7, Electromagnetic compatibility (EMC), Part 4-7: Testing and measurement techniques – General guide on harmonics and interharmonics measurements and instrumentation, for power supply and equipment connected thereto.

15. IEC-61000-4-30, Electromagnetic compatibility (EMC), Part 4-30: Testing and measurement techniques – Power quality measurement methods.